

## SUB-BANDGAP LASER PROBING OF GaAs DEVICES AND CIRCUITS

D.M.Mechtél, A.G.Andreou, D.N.Christodoulides  
J.Wagner, C.R.Westgate, and C.H.Palmer

The Johns Hopkins University  
34th and Charles Streets  
Baltimore, MD 21218

T.O. Poehler

Applied Physics Laboratory  
Johns Hopkins Road  
Laurel, MD 20707

### INTRODUCTION

Standard methods for measuring solid-state device and circuit performance are inadequate at GHz speeds because they introduce parasitic inductances and capacitances that change circuit operation and characteristics. One promising noninvasive procedure that avoids these problems uses electro-optic probing to yield information on device packaging techniques; and on device and circuit performance characteristics such as voltage waveforms, timing, and propagation delays in both analog and digital circuits.

This review includes three topics: a discussion of the limitations of standard test methods at GHz speeds, a description of the basic principles of electro-optic probing, and a review of some of the applications of electro-optic probing.

### LIMITATIONS OF STANDARD TEST METHODS

Standard test methods fail to measure accurately the performance of circuits operating at high speeds. For example, the temporal resolution of sampling oscilloscopes, which are frequently used for high speed testing, is limited to about 25 ps [1]. Network analyzers are standard instruments for measuring small-signal S-parameters in microwave analog circuits. The frequency response of most commercially available network analyzers is also limited (40 GHz) [2].

Both sampling oscilloscopes and network analyzers can probe terminal nodes. A test instrument that probes signals in the circuit was recently marketed [3]. Nevertheless, it requires special test structures and the probe introduces some parasitics.

Electro-optic probing permits internal circuit measurements without introducing parasitics and improves on traditional test methods in both temporal and spatial resolution.

### PRINCIPLES OF ELECTRO-OPTIC PROBING

Electro-optic probing is based on the linear electro-optic effect: the change in the index of refraction of a crystal in the presence of an electric field. The simplified schematic in

Figure 1, illustrates the basic principles of electro-optic probing of the electric field along a microstrip transmission line. Microstrip is a two conductor microwave transmission line constructed on semi-insulating GaAs in this case. The [100] and [001] directions of the GaAs crystal are oriented along the x and z axes respectively. GaAs belongs to a class of crystals that lack inversion symmetry and thus exhibits the linear electro-optic effect [4]. Further information on crystal structure may be found in reference [5].

The light source and polarizer in Figure 1 produce light linearly polarized in the y direction to probe the voltage along the transmission line. The area probed is defined by the diameter of the light beam incident on the microstrip sample and hence is diffraction limited. In the GaAs crystal, the linearly polarized light is split into two polarization components and each component experiences a different index of refraction. As a result, a phase delay, that is related to the strength of the electric field at the probed point, is introduced between the components. Passage through an analyzer converts the phase delay to a change in the light intensity that can be measured by a photodetector. The detected light intensity is a function of the voltage along the microstrip transmission line at the point probed. The quarter-wave plate biases the system to optimize system performance.

In Figure 1, the bottom conductor must be thin enough to be transparent to light. In practice, other testing geometries have been used for various test samples. Figure 2 shows two typical testing geometries: front side probing where the bottom conductor reflects the light beam, and back side probing where the top conductor reflects the light beam [6]. Since both geometries require a double pass through the GaAs sample, the measurement is more sensitive than the single pass probing illustrated in Figure 1 [1].

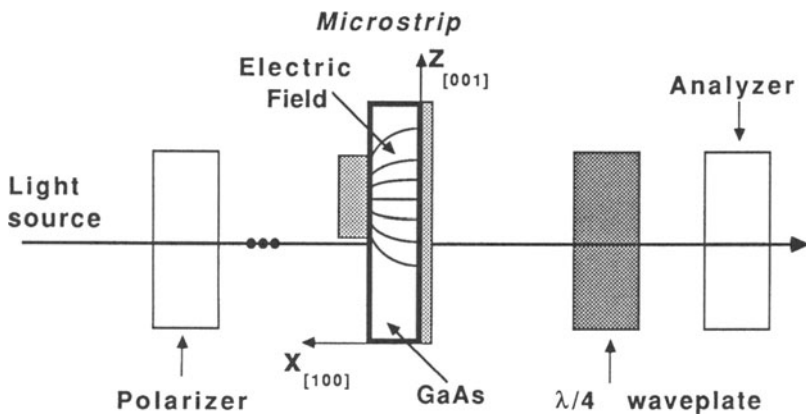


Fig 1. Electro-optic probing

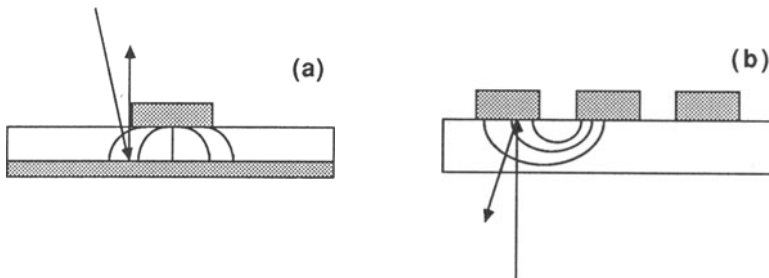


Fig 2. Testing geometries (a) front side probing (b) back side probing

The effect of the electric field on the indices of refraction of GaAs is easily illustrated by the index ellipsoid for GaAs. Given the direction of the wave normal of the propagating light incident on the crystal, the index ellipsoid has the following property. The intersection of the index ellipsoid and a plane perpendicular to the wave normal is an ellipse. The two allowable directions of polarization associated with the wave normal coincide with the directions of the major and minor axes of the ellipse. The magnitudes of the radius vectors along the ellipse axes give the indices of refraction for the two polarization directions [7]. A general analysis of the index ellipsoid may be found in references [5,8].

GaAs is a cubic crystal so its index of refraction is isotropic and its index ellipsoid is a sphere. GaAs's index of refraction  $n_o$  changes in an electric field deforming the index ellipsoid from its spherical shape. This deformation is the basis of electro-optic probing.

The general equation for an ellipsoid with constants  $a_{ij}$  is

$$a_{11}x^2 + a_{22}y^2 + a_{33}z^2 + 2a_{23}yz + 2a_{31}zx + 2a_{12}xy = 1. \quad (1)$$

For GaAs in the absence of an electric field, equation (1) becomes

$$\frac{x^2}{n_o^2} + \frac{y^2}{n_o^2} + \frac{z^2}{n_o^2} = 1. \quad (2)$$

The deformation of the spherical index ellipsoid for GaAs because of an electric field changes the coefficients in equation (2). The change in each coefficient  $a_{ij}$  is related to each component of the electric field  $E$  by the electro-optic matrix for GaAs where  $r_{kl}$  is an electro-optic coefficient [7].

$$\begin{bmatrix} \Delta a_{11} \\ \Delta a_{22} \\ \Delta a_{33} \\ \Delta a_{23} \\ \Delta a_{31} \\ \Delta a_{12} \end{bmatrix} = \begin{bmatrix} 0 & 0 & 0 \\ 0 & 0 & 0 \\ 0 & 0 & 0 \\ r_{41} & 0 & 0 \\ 0 & r_{41} & 0 \\ 0 & 0 & r_{41} \end{bmatrix} \begin{bmatrix} E_x \\ E_y \\ E_z \end{bmatrix}. \quad (3)$$

The ellipsoid produced by the deformation of the sphere is described by

$$\frac{x^2}{n_o^2} + \frac{y^2}{n_o^2} + \frac{z^2}{n_o^2} + 2r_{41}E_xyz + 2r_{41}E_yzx + 2r_{41}E_zxy = 1. \quad (4)$$

For Figure 1,  $E_y = E_z = 0$  since the light beam only interacts with the x component of the electric field, hence equation (4) becomes

$$\frac{x^2}{n_o^2} + \frac{y^2}{n_o^2} + \frac{z^2}{n_o^2} + 2r_{41}E_xyz = 1. \quad (5)$$

A 45° rotation about the x axis transforms equation (5) into a convenient form for determining the index of refraction for each of the two allowable polarization components:

$$\frac{x'^2}{n_o^2} + \frac{y'^2}{\left[n_o + \frac{n_o^3}{2}r_{41}E_x\right]^2} + \frac{z'^2}{\left[n_o - \frac{n_o^3}{2}r_{41}E_x\right]^2} = 1. \quad (6)$$

In Figure 1, the light in the GaAs sample is polarized along the  $y'$  and  $z'$  axes as defined in

equation (6). The indices of refraction for its polarization components are:

$$n_{y'} = n_o + \frac{n_o^3}{2} r_{41} E_x \quad (7)$$

$$n_{z'} = n_o - \frac{n_o^3}{2} r_{41} E_x . \quad (8)$$

The phase delay  $\Gamma$  introduced by light passing through the GaAs is

$$\Gamma = \Theta_{z'} - \Theta_{y'} = \frac{2\pi}{\lambda} n_o^3 r_{41} V \quad (9)$$

where  $\Theta$  is the phase,  $\lambda$  is the wavelength of the incident light, and  $V$  is the voltage signal probed in the test sample.

The half-wave voltage  $V_\pi$  is the voltage level in the test sample that corresponds to a phase delay of  $\pi$ . Using this definition, equation (9) becomes

$$\Gamma = \frac{\pi V}{V_\pi} . \quad (10)$$

For the two polarizer, quarter-wave plate test system in Figure 1, the ratio of output to input light intensity  $I_o / I_i$  is related to the voltage signal at the GaAs microstrip sample point by

$$\frac{I_o}{I_i} = \frac{1}{2} \left[ 1 + \sin \left( \frac{\pi V}{V_\pi} \right) \right] . \quad (11)$$

The graphical representation of equation (11) in Figure 3 illustrates that the electro-optic probing system operates with greatest sensitivity near  $1/2$  the half-wave voltage. The quarter-wave plate optically biases the system for operation at that point.

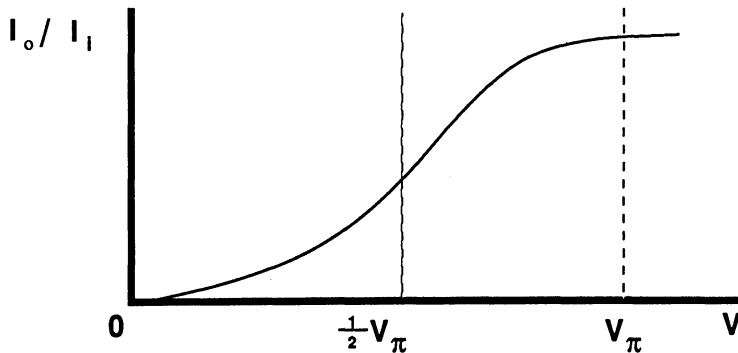


Fig 3. Intensity ratio vs. Sample voltage

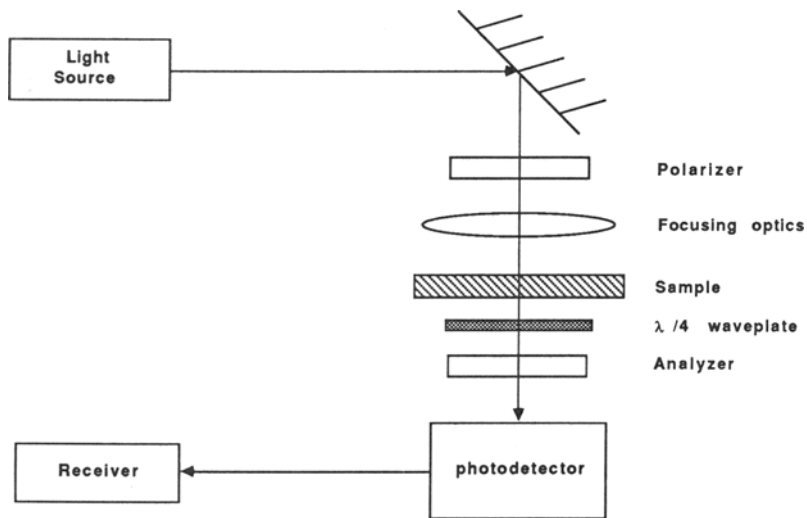


Fig 4. Generic electro-optic probing test setup

## APPLICATIONS

A general schematic of an electro-optic probing system is shown in Figure 4. The technique is intended to be noninvasive, so the light source energy must be below the bandgap of GaAs (1.424eV [9]) ensuring that photocarriers are not generated by the light incident on the test sample. In practice, the laser should have a wavelength of  $1\ \mu\text{m}$  or greater. The output current of the illuminated photodetector is connected to a receiver.

Electro-optic probing has been carried out with two different techniques: continuous wave probing and pulsed probing.

The first experiment with continuous wave probing determined the electric field in a GaAs coplanar waveguide sample [10]. Figure 5 shows a general diagram of the experimental setup. The light source was an InGaAsP CW semiconductor laser ( $\lambda=1.3\ \mu\text{m}$ ) and the optical train was similar to that in Figure 1 except for added focusing optics and a back side probing geometry. The detection system was a photodetector coupled with a lock-in amplifier. The system's spatial resolution was about  $12.5\ \mu\text{m}$ .

Later work defined the surface potential in GaAs samples with continuous wave probing [11]. Three-dimensional mapping of the electric field distribution by continuous wave probing has been proposed and preliminary experimental results have been obtained [12]. These results show that this probing technique can determine field and charge distributions in GaAs devices and circuits.

The first picosecond electro-optic probing or sampling measurement made directly in GaAs used pulsed probing [13]. Then, the first electro-optic sampling measurement directed to the interior points of a GaAs integrated circuit was demonstrated with a front-side probing geometry [14]. In this test, the voltage levels of the gate and drain lines of a GaAs FET Traveling Wave Amplifier (TWA) were probed. Figure 6 shows a schematic diagram of the experimental setup. A mode-locked Nd:YAG laser ( $\lambda=1.06\ \mu\text{m}$ ) emitting 100 ps pulses at 82 MHz coupled with a fiber-grating pulse compressor that limited the pulse length to 10 ps provided the sampling pulses. The fixed frequency receiver was a spectrum analyzer and a photodiode was the light detector. The microwave signal source that drove the IC was synchronized with the mode-locked laser by tuning the microwave signal to the Nth harmonic

of the pulse repetition rate so that each point of the voltage signal transmitted on the gate and drain lines was sampled every Nth cycle. This technique is similar to a sampling oscilloscopes' measurement process. The complete waveform is mapped out by varying the phase of the external microwave signal generator.

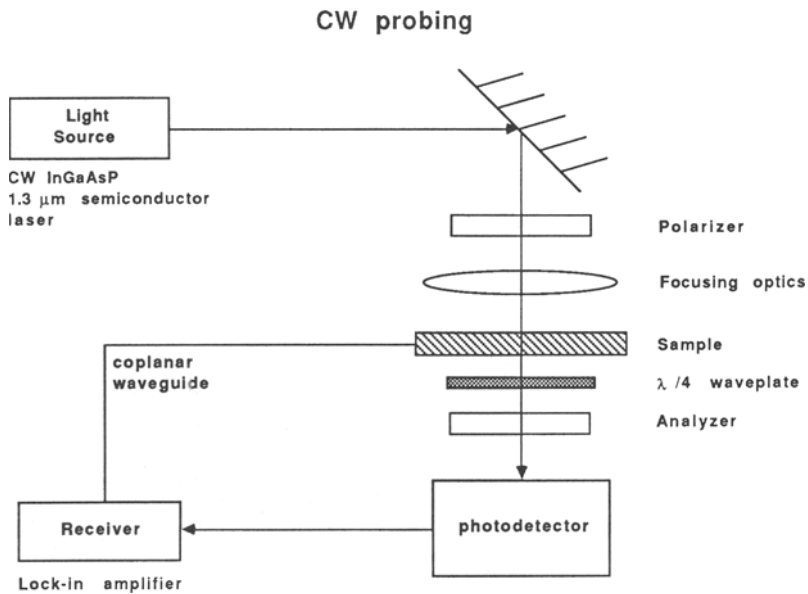


Fig 5. Experimental Setup

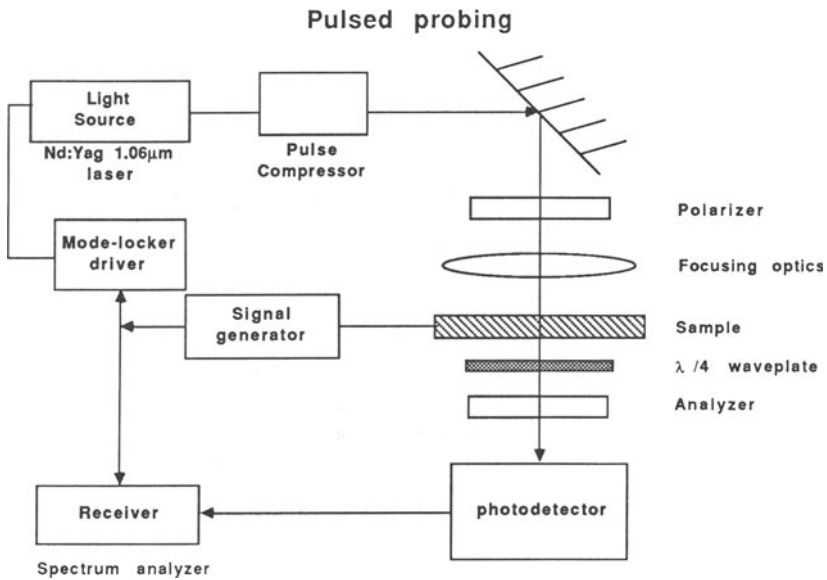


Fig 6. Experimental Setup

Pulsed probing is more expensive and complicated than continuous wave probing. Pulsed probing introduces the problem of phase stability between the laser and the external signal sources. In the system described above, a phase-locked loop reduced the timing jitter from 10 ps RMS to 1.5 ps RMS. The temporal resolution, which is a function of the sampling pulse width, was 10 ps. A description of other resolution limits and an excellent review of pulsed probing may be found in reference [1].

Other work measured voltage levels in planar GaAs digital circuits with the back side probing geometry [6]. The switching delays in combinational logic GaAs integrated circuits and the timing of sequential logic circuits have also been tested [15].

The pulsed probing system of reference [14] was improved so that the feedback system reduced timing jitter to .5 ps RMS. In addition, the pulse compressor shortens the pulses to 1.5 ps FWHM thereby improving the temporal resolution [16].

Other testing methods for GaAs have been developed such as a synchronized two-pulse output system. In one experiment, one pulse stimulated a GaAs photodiode and the other recorded the waveform [13]. The stimulating pulse, with a wavelength of 532 nm, is above the bandgap of GaAs. The sampling pulse had a 1.06  $\mu\text{m}$  wavelength. A variation of this technique was used to excite and probe digital GaAs integrated circuits measuring the single-gate propagation delays of logic gates within the integrated circuits [17].

Finally, Andreou and Christodoulides have proposed a novel optical probe to measure mobility in electro-optic materials [18]. Since Hall-effect-induced birefringence has been recently demonstrated in GaAs [19], this probe permits new applications for sub-bandgap probing of GaAs devices to study the electronic transport and hot-carrier dynamics. The probe can also make high resolution noninvasive mobility measurements in electro-optic crystals.

The applications described above illustrate how electro-optic probing makes internal measurements in both analog and digital GaAs circuits. The spatial resolution is limited only by the diameter of the probe beam incident on the test sample. The temporal resolution of electro-optic sampling systems steadily improves as the pulse width is shortened.

As electro-optic probing is further developed, it will be routinely applied to the testing of microwave integrated circuits.

## REFERENCES

1. B.H. Kolner and D.M. Bloom, *IEEE J. Quantum Electron.* **QE-22**, 79 (1986)
2. Hewlett Packard, Measurement Computation Systems Catalog
3. D. E. Carlton, K.R. Gleason, and E.W. Strid, Test and Measurement World, May 1985
4. A. Yariv, *Optical Electronics* (Holt, Rinehart, and Winston, New York, 1985)
5. J.F. Nye, *Physical Properties of Crystals* (Oxford University Press, London, 1957)
6. J.L. Freeman, S.K. Diamond, H. Fong, and D.M. Bloom *Appl. Phys. Lett.* **47**, 1083 (1985)
7. K. Iizuka, *Engineering Optics*, (Springer-Verlag, New York, 1983)
8. I.P. Kaminow, *An Introduction to Electrooptic Devices* (Academic Press, New York, 1974)
9. S.M. Sze, *Physics of Semiconductor Devices*, (John Wiley and Sons, New York, 1981)
10. Z. H. Zhu, J.P. Weber, S.Y. Wang, and S. Wang, *Appl. Phys. Lett.* **49**, 432 (1986)
11. Y.H. Lo, Z.H. Zhu, C.L. Pan, S.Y. Wang, and S. Wang, *Appl. Phys. Lett.* **50**, 1125 (1987)
12. Y.H. Lo, M.C. Wu, Z.H. Zhu, S.Y. Wang, and S. Wang, *Appl. Phys. Lett.* **50**, 1791 (1987)
13. B.H. Kolner and D.M. Bloom, *Electron. Lett.* **20**, 818 (1984)
14. K.J. Weingarten, M.J.W. Rodwell, H.K. Heinrich, B.H. Kolner, and D.M. Bloom, *Electron. Lett.* **21**, 765 (1985)

15. M.J.W. Rodwell, K.J. Weingarten, J.L. Freeman and D.M. Bloom, *Electron. Lett.* **22**, 499 (1986)
16. K.J. Weingarten, M.J.W. Rodwell, and D.M. Bloom, to appear in Picosecond Electronics and Optoelectronics, edited by G. Mourou, D.M. Bloom, and C.-H. Lee (Springer-Verlag, New York)
17. X.-C. Zhang and R.K. Jain, *Electron. Lett.* **22**, 264 (1986)
18. A.G. Andreou and D.N. Christodoulides, "A novel optical probe to measure mobility in electro-optic materials" Dept. of Elec. and Comp. Engr., The Johns Hopkins University Technical Report JHU/ECE-87/15
19. A.G. Andreou, D.N. Christodoulides, T.O. Poehler, and C.R. Westgate, "Hall-effect-induced birefringence in GaAs" in preparation